Nagra
Nationale
Genossenschaft
für die Lagerung
radioaktiver Abfälle

Cédra
Société coopérative
nationale
pour l'entreposage
de déchets radioactifs

Cisra
Società cooperativa
nazionale
per l'immagazzinamento
di scorie radioattive

TECHNICAL REPORT 85-51

Determination of crack growth parameters of alumina in 4-point bending tests

T. Fett[1]
K. Keller[2]
D. Munz[3]

September 1985

[1] Institut für Material- und Festkörperforschung IV, Kernforschungszentrum Karlsruhe
[2] Institut für Keramik im Maschinenbau, Universität Karlsruhe
[3] Institut für Zuverlässigkeit und Schadenskunde im Maschinenbau, Universität Karlsruhe

Parkstrasse 23 5401 Baden/Schweiz Telephon 056/20 55 11

Nagra
Nationale
Genossenschaft
für die Lagerung
radioaktiver Abfälle

Cédra
Société coopérative
nationale
pour l'entreposage
de déchets radioactifs

Cisra
Società cooperativa
nazionale
per l'immagazzinamento
di scorie radioattive

TECHNICAL REPORT 85-51

Determination of crack growth parameters of alumina in 4-point bending tests

T. Fett[1]
K. Keller[2]
D. Munz[3]

September 1985

1) Institut für Material- und Festkörperforschung IV, Kernforschungszentrum Karlsruhe
2) Institut für Keramik im Maschinenbau, Universität Karlsruhe
3) Institut für Zuverlässigkeit und Schadenskunde im Maschinenbau, Universität Karlsruhe

Parkstrasse 23 5401 Baden/Schweiz Telephon 056/20 55 11

SUMMARY

Alumina containers are being considered for the disposal of nuclear waste in a number of countries. For this ceramic material subcritical crack growth is an potentially important failure mechanism.

The crack growth behaviour of one particular type of hot isostatically pressed alumina has been investigated at 70°C in a strongly corrosive brine using fracture-mechanical methods. The use of a recently developed method for interpreting lifetime measurements in static bending tests allowed a determination of crack growth rates as low as 10^{-11} m/s.

It was observed that the dependence of the crack growth rate on the stress intensity factor can be described in terms of a power low over the whole range investigated. The exponent in the power law was found to be close to n = 20. Published values for the same material, determined by the double torsion method, lie above n = 100. The discrepancy between these values is probably due to R-curve effects (i.e. to an increase of the critical stress intensity factor in the course of crack extension) that influence the behaviour of macroscopic cracks and that of natural cracks about 100 μm in size differently.

Because of the high lifetime required of containers for final disposal of radioactive waste the low values determined for the crack growth exponent imply that tensile stresses must be kept quite small.

ZUSAMMENFASSUNG

Für die nukleare Entsorgung werden in einigen Ländern Endlagerbehälter aus Aluminiumoxid in Erwägung gezogen. Bei diesem keramischen Material ist unterkritische Rissausbreitung ein wichtiger potentieller Versagensmechanismus.

Es wurde ein heissisostatisch gepresstes Al_2O_3 hinsichtlich seines Risswachstumsverhaltens in einer stark korrosiven Salzlösung bei 70°C mit bruchmechanischen Methoden untersucht. Durch eine neuartige Auswertung von Lebendauermessungen im statischen Biegeversuch konnten Risswachstumsgeschwindigkeiten bis zu 10^{-11} m/s gemessen werden.

Dabei zeigte es sich, dass die Abhängigkeit der Risswachstumsgeschwindigkeit vom Spannungsintensitätsfaktor über den gesamten Messbereich durch ein Potenzgesetz beschrieben werden kann. Es wurde ein Risswachstumsexponent von $n=20$ gefunden. Aus der Literatur sind für das gleiche Material - aufgrund von Messungen mit der Doppel-Torsionsmethode - Werte $n > 100$ bekannt. Die Diskrepanz zwischen diesen Ergebnissen ist wahrscheinlich auf R-Kurven-Effekte (d.h. auf eine Zunahme des Bruchwiderstands mit fortschreitender Rissausbreitung) zurückzuführen, welche das Verhalten von Makrorissen und natürlichen Rissen in der Grössenordnung von ca. 100 μm unterschiedlich beeinflussen.

Bei den hohen anzustrebenden Lebensdauern von Endlagerbehältern führt der niedrige gemessene Wert des Risswachstumsexponenten zu recht tiefen Werten für die zulässigen Zugspannungen.

RESUME

Dans plusieurs pays on étudie la possibilité d'utiliser des conteneurs en alumine pour l'entreposage final des déchets radioactifs. Dans ce type de matériaux céramiques la croissance sous-critique des fissures représente un mécanisme important pouvant conduire à la rupture du conteneur.

On a étudié, par les methodes de la mécanique de la rupture, la propagation des fissures, à 70°C et dans une solution fortement corrosive, dans un type particulier d'alumine pressé isostatiquement à chaud. A l'aide d'une méthode récemment développée d'évaluation des essais de durée de vie sous flexion, on a pu mesurer des taux de propagation de fissure allant jusqu'à 10^{-11} m/s.

On a constaté que la vitesse de propagation des failles est proportionnelle au facteur d'intensité à la puissance $n \cong 20$, dans l'ensemble du domaine considéré. Dans la littérature on trouve des valeurs $n > 100$ obtenues antérieurement pour le même matériau par la méthode de double torsion. Il est probable que la discrépance entre ces deux résultats est due à des effets de courbe R (c.-à-d. à une augmentation du facteur critique d'intensité au cours de la propagation de la fissure): cet effet aurait une influence sur le comportement des macrofissures différente de celle qu'il a sur la propagation des fissures naturelles, de l'ordre de grandeur de 100 μm.

Si l'on tient compte de la durée de vie requise pour un conteneur pour l'entreposage final de déchets radioactifs, on constate que la faible valeur mesurée pour l'exposant de croissance impose de limiter fortement les contraintes en tension.

CONTENTS Page

1. INTRODUCTION

For ultimate storage of high level waste, the use of aluminium oxide as container material is being considered in several countries. This type of containers might fail due to corrosion, buckling and by exceeding the tensile strength or subcritical crack growth because tensile stresses cannot be excluded. Since water will affect the container surface and lifetimes of the order of 1000 years are required, it seems that subcritical crack growth of preexisting surface cracks is the most serious potential failure mechanism. This study deals with the subcritical crack growth behaviour of a hot isostatically pressed alumina envisaged for ultimate storage purposes /1/. As fracture in ceramics usually starts at a defect introduced in the course of fabrication or processing, it is necessary to study the crack growth phenomenon starting from natural cracks.

2. FUNDAMENTAL EQUATIONS

In case of linear-elastic material behaviour crack growth is governed by the stress intensity factor K_I, defined by

$$K_I = \sigma \sqrt{a}\, Y \tag{1}$$

where a is the size of a crack and Y is a geometric correction factor dependent on the shape of the crack and of the specimen.
If $v(K_I)$ is the crack growth rate

$$\frac{da}{dt} = v(K_I) \tag{2}$$

the lifetime of a specimen with a surface crack, by combination of Eqs. (1) and (2), becomes

$$t_f = \frac{2}{Y^2 \sigma^2} \int_{K_{Ii}}^{K_{Ic}} \frac{K_I \, dK_I}{v(K_I)} \tag{3}$$

where

$$K_{Ii} = \sigma \sqrt{a_o}\, Y \tag{4}$$

is the initial value of the stress intensity factor. It is assumed that Y is independent of crack length between a_o and the critical crack length a_c. By definition K_{Ic} is the fracture toughness. It is often observed that the dependency of $v(K_I)$ on K_I takes the form of a power law over a wide range of growth rates:

$$v(K_I) = A K_I^n \tag{5}$$

In this case one obtains for $K_{Ii}^{n-2} << K_{Ic}^{n-2}$

$$t_f = B \sigma_c^{n-2} \sigma^{-n} \tag{6}$$

with

$$B = \frac{2}{AY^2(n-2)K_{Ic}^{n-2}} \tag{7}$$

and the strength σ_c in the absence of subcritical crack growth

$$\sigma_c = \frac{K_{Ic}}{Y\sqrt{a_o}} \tag{8}$$

The distribution of ceramic strength values can often be described by a Weibull distribution. For the bending strength in an inert medium, σ_c, the cumulative frequency F, i.e. the probability that the actual strength of a randomly chosen sample lies below σ_c, is given according to the equation

$$F = 1 - \exp[-(\sigma_c/\sigma_o)^m] \tag{9}$$

where m and σ_o are the Weibull parameters.
In a logarithmic plot according to

$$\ln\ln 1/(1-F) = m \ln(\sigma_c/\sigma_o) = m \ln \sigma_c - m \ln \sigma_o \tag{10}$$

a straight line with the slope m results.

Substituting t_f for σ_c using Eq. (6) results in a Weibull-distribution for the time to failure with the cumulative frequency

$$F = 1 - \exp[-(t_f/t_o)^{m^*}] \tag{11}$$

with

$$m^* = \frac{m}{n-2} \tag{12a}$$

and

$$t_o = B \sigma_o^{n-2} \sigma^{-n} \tag{12b}$$

3. METHODS OF DETERMINATION OF SUBCRITICAL CRACK GROWTH

In recent years various methods have been developed to determine the v-K_I-behaviour.

a) Double-Torsion-method (DT)

The advantages of this most popular method are:
- Crack extension can be observed under the microscope or in an indirect manner by compliance measurements.
- A complete v-K_I-curve can be determined with, in principle, only one specimen.

Disadvantages with respect to lifetime predictions are:
- Crack growth rates are limited by $v > 10^{-9}$ m/s /2/.
- DT-measurements are carried out with cracks of the order of several mm, but for lifetime predictions the crack growth behaviour of natural cracks of the order of 50 μm is of interest. The extrapolation of the results to natural crack sizes is not always possible /3/.
- Especially for materials with a strong R-curve effect (i.e. materials exhibiting an increase of K_{Ic} in the course of the crack extension) DT-measurements are not appropriate to predict the behaviour of small natural cracks where R-curve effects are negligible /4/.

b) Dynamic bending tests

From measurements of bending strengths at different stress rates one can evaluate n and B (or A) /5/.

Advantages of this procedure are:
- The test method is very simple and only a simple equipment is necessary.
- Crack growth data are determined with specimens containing natural cracks and therefore problems of transferability are eliminated.

The disadvantages are:
- The type of v-K_I relation has to be known.
- Inevitably, the bending strength is affected mainly by crack growth at a relatively high crack growth rate so that the crack growth parameters obtained are not necessarily characteristic of those crack growth rates which are of interest for lifetime predictions.

c) Crack growth data evaluated from lifetime measurements in static bending tests

From lifetime measurements performed at different bending stresses n and B can be determined by plotting $\lg(t_f)$ versus $\lg(\sigma)$ using Eq. (6) or by evaluating the Weibull parameter m using Eq. (12a).

The advantages of this method - apart from those mentioned under b) - are:
- Lifetime predictions require only extrapolation of the measured lifetimes.

- The crack growth rates which appear in lifetime measurements can be distinctly lower than those resulting from DT-measurements.

Disadvantage:
- For integration a particular type of v-K_I dependency has to be assumed and its accuracy can be judged in a supplementary step only.

d) Determination of v-K_I-relations from lifetime measurements

A modified procedure for the evaluation of crack growth rates from lifetime measurements is proposed in /6/. This method does not require the v-K_I dependency to be known.

The principle is to load a series of samples with a constant stress σ. By differentiation of Eq. (3) with respect to the initial stress intensity factor K_{Ii} one obtains

$$\left.\frac{dt}{dK_{Ii}}\right|_{\sigma=\text{const}} = -\frac{2\,K_{Ii}}{Y^2\sigma^2 v(K_{Ii})} \tag{13}$$

Inserting logarithmic derivatives

$$t_f\, d(\ln t_f) = dt_f \quad ; \quad K_{Ii}\, d(\ln K_{Ii}) = dK_{Ii}$$

yields

$$\frac{d(\ln t_f)}{d(\ln K_{Ii})} = -\frac{2\,K_{Ii}^2}{Y^2\sigma^2 t_f\, v(K_{Ii})} \tag{14}$$

and, consequently, the crack growth rate attached to K_{Ii} becomes

$$v(K_{Ii}) = -\frac{2\,K_{Ii}}{Y^2\sigma^2 t_f}\;\frac{d(\ln K_{Ii})}{d(\ln t_f)} \tag{15}$$

In the special case of a power law one has

$$\frac{d(\ln t_f)}{d(\ln K_{Ii})} = n-2$$

As

$$K_{Ii}/K_{Ic} = \sigma/\sigma_c \tag{16}$$

one obtains

$$v(K_{Ii}/K_{Ic}) = -\frac{2\,K_{Ic}^2}{Y^2\sigma_c^2 t_f}\;\frac{d(\ln K_{Ii}/K_{Ic})}{d(\ln t_f)} \tag{17}$$

The procedure is relatively simple. In a first series of tests N samples are loaded with a given stress σ. The N values of lifetimes are ranked in increasing order. A second series also involving N specimens is tested in dynamic bending tests at high stress rates in an inert environment to give the distribution of socalled "inert strength". These values are similarly ranked in increasing order. The ν-th value of lifetime $t_{f,\nu}$ is associated with the ν-th value of inert bending strength $\sigma_{c,\nu}$. The latter is transformed to $K_{Ii,\nu}/K_{Ic}$ using Eq. (16), with σ from constant load tests.

By plotting $t_{f,\nu}$ versus $K_{Ii,\nu}/K_{Ic}$ one obtains the dependency depicted schematically in Figure 1. Using a suitable smoothing procedure, one can determine $d(\ln t_f)/d(\ln K_{Ii}/K_{Ic})$ for each value of K_{Ii}/K_{Ic}. From Eq. (17) the accompanying v-K_I-curve of Figure 2 results.

4. EXPERIMENTAL INVESTIGATIONS

4.1 Dynamic bending strength

Bending bars, 3.5x4.4x45mm, cut out from a hot isostatically pressed Al_2O_3-container (manufactured by ASEA, Sweden) were made available by NAGRA, Switzerland. The surface roughness is characterized by a mean value of peak to valley height of 0.27 μm and corresponding maximum value of 3.5 μm. The crack growth parameters of these specimens were to be determined and lifetime predictions made for some postulated tensile stresses. A salt solution (based on NAGRA AN/84-61) was specified as the test environment. The concentration in mg/l was

$NaCl$	8297
KCl	86
$MgCl_2\ 6H_2O$	22
$SrCl_2\ 6H_2O$	64
NaF	8
$NaHCO_3$	84
$CaCl_2\ 2H_2O$	3191
Na_2SO_4	2307

Prior to testing the Al_2O_3 specimens were annealed for 2 hours at 1150°C under vacuum conditions (10^{-5}bar). To determine the inert bending strength σ_c a sample of 15 specimens was subjected to dynamic 4-point bending tests with a 20 mm inner span and a 40 mm outer span in air and a high stress rate of $\dot{\sigma}$ = 350 MPa/s. The result is shown in Fig. 3 in a Weibull plot. For this purpose, the N strength values were arranged in ascending order and the cumulative distribution function $F = i/(N+1)$ was allocated to the i^{th} value of σ_c. The results were plotted as $\ln\ln 1/(1-F)$ vs σ_c according to Eq. (10). The results of measurement were evaluated using the maximum likelihood method /7/ and they yielded the data

$$m = 10.4 \qquad \sigma_o = 369 \text{ MPa}$$

The median value of the inert bending strength - i.e. the value corresponding to F = 0.5 - is $\hat{\sigma}_c$ = 355 MPa.

4.2 Lifetime measurements

Lifetime measurements were performed in static 4-point bending tests at 70°C in the salt solution specified in Section 4.1. The lifetimes obtained for different bending stresses are represented in Fig. 4. The bending stresses applied were 217, 173, 155 and 140 MPa. Lifetime tests exceeding a limit of 400 hours were discontinued and classified as "runthroughs". Only at the lowest load 5 runthroughs were observed. A Weibull analysis using the maximum likelihood method gives the following Weibull parameters m* and median values $\hat{t}_f$ - i.e. the lifetimes at F = 0.5 -:

Table 1

σ	m^*	$\hat{t}_f$
217 MPa	0.808	244 s = 0.068 h
173 MPa	1.316	38900 s = 10.8 h
155 MPa	0.861	1.41×10^5 s = 39.06 h
140 MPa	-	1.58×10^6 s = 440.2 h

The median lifetime $\hat{t}_f$ for σ = 140 MPa was evaluated by extrapolation of the three lifetime data.

5. DETERMINATION OF CRACK GROWTH BEHAVIOUR

In Fig. 5 the median values of lifetime $\hat{t}_f$ are plotted versus the bending stress applied. From the slope of the fitted straight line one obtains n by using Eq. (6) in a logarithmic formulation

$$\ln \sigma = \frac{1}{n} \ln (B \tilde{\sigma}_c^{n-2}) - \frac{1}{n} \ln \hat{t}_f \tag{18}$$

(slope = - 1/n), as

$$n = 20$$

For a lifetime of t_f = 1 h one can conclude a corresponding applied stress σ = 188.3 MPa. Eq. (18) yields

$$\ln (B \tilde{\sigma}_c^{n-2}) = 104.76 \quad ; \quad B = 0.3914 \ \mathrm{MPa}^2 \mathrm{h}$$

A second method of evaluating n is based on Eq (12a). By use of m = 10.4 and the m*-data reported in Table 1 one obtains

Table 2

σ	n
217 MPa	14.9
173 MPa	9.9
155 MPa	14.1

The mean value of $\bar{n}$ = 13 confirms the relatively low n-value obtained by evaluation of Fig. 5.

In addition, the crack growth behaviour is analysed employing the method reported in Section 3b. Even if the distributions of the inert bending strength or the lifetime can only be described approximately by a Weibull distribution, the crack growth rates can still be derived from the individual strength and lifetime values. The procedure is also independent of the validity of Eqs. (5) and (6).

Figure 6 shows all measured lifetimes in dependence of the normalized stresses σ/σ_c. For each of the three test series the slope $d\ln(K_{Ii}/K_{Ic})/d\ln t_f$ were determined. The investigated material showed straight lines. For each measured lifetime t_f the related inert strength σ_c corresponding to the same cumulative frequency is known. Then the v-K_I-data can be computed by application of Eq. (17) using $Y=2/\sqrt{\pi}$, K_{Ic} = 4 MPa$\sqrt{m}$ /8/. The v-K_I dependency is depicted in Fig. 7. It can be expressed by a power law down to crack growth rates of 10^{-11} m/s. The fitted straight line is drawn in Fig. 7 and shows an exponent n = 19 and B = 0.59 MPa^{2}h in good agreement to the value obtained from Fig. 5.

6. COMPARISON WITH LITERATURE DATA

Since n, B, m and σ_o are known, it is possible to make lifetime predictions. The magnitude of n is of very high importance for such predictions because $t_f \sim \sigma^{-n}$. For the investigated material n-values of the order of 200 and more were reported in /9/ in contrast to the data found in this investigation. The data of /9/ were obtained by Double-Torsion (DT) measurements carried out in so-called "Groundwater 1", which is representative of conditions in the Swedish granitic bedrock.

Deuerler, Knehans and Steinbrech /4/ have shown that ceramics with R-curve behaviour (i.e. K_{Ic} increases with crack extension) yield incorrect n-values if macroscopic cracks are taken into account. In the course of extension of large cracks (of the order of mm) the increasing K_{Ic} affects the n-values. In their experiments the authors found n > 150. After elimination of the influence of R-curve behaviour the crack growth exponent n - describing pure subcritical crack growth - became n ≈ 41. This was in good agreement with dynamic bending tests where n ≈ 50 was found.

7. LIFETIME PREDICTIONS

Lifetime predictions can be made by use of Eq. (6) and Eq. (10). From Eq. (10) it follows

$$\sigma_c = \sigma_o \exp\left[\frac{1}{m}\ln\ln 1/(1-F)\right] \qquad (19)$$

and by insertion into Eq. (6), one obtains

$$t_f = B\,\sigma_o^{n-2} \exp\left[\frac{n-2}{m} \ln\ln 1/(1-F)\right] \sigma^{-n} \tag{20}$$

For ultimate storage container an admissable failure probability of $F = 10^{-3}$ is assumed. Two questions are of interest:

a) A minimum lifetime of 1000 years is required. What are the allowable tensile stresses?
Insertion of $F = 10^{-3}$, $n = 20$, $m = 10.4$, $B = 0.3914\ \mathrm{MPa^2\,h}$, $t_f = 8.76 \cdot 10^6\ \mathrm{h}$ and $\sigma_o = 369$ MPa gives by use of Eq. (20)
$\sigma_{max} = 48.2$ MPa

b) In the second question residual stresses σ_{res} caused by manufacture are supposed. The expected lifetime is:

1. $t_f = 4.4 \cdot 10^{10}$ years for $\sigma_{res} = 20$ MPa
2. $t_f = 6.1 \cdot 10^5$ years for $\sigma_{res} = 35$ MPa
3. $t_f = 484$ years for $\sigma_{res} = 50$ MPa

Relation (20) is represented in Fig. 8 and the examples are marked in it.

The lifetime predictions mentioned in this chapter are performed for specimen of constant sizes. It is known that strength and lifetime will decrease if volumina and surface of predicted construction are larger than those of measured bending specimens. Consequently, the allowable stresses and attainable lifetimes become lower. For exact calculations the stress distribution in the container wall has to be known.

8. INFLUENCE OF SURFACE ROUGHNESS ON BENDING STRENGTH

As mentioned in Section 1. the surface roughness was characterized by a maximum peak-to-valley height of 3.5 μm and a corresponding mean value of 0.27 μm. It was of interest to know the influence of the surface quality on the inert bending strength. Therefore, three surfaces of a series of bending bars were polished which produced a maximum peak-to-valley height of 0.046 μm and a mean roughness of only 0.004 μm. After annealing under vacuum conditions the inert bending strength was measured again. As shown in Fig. 9, an increment of approximatively 40% in bending strength can be observed, but the Weibull modulus m is hardly influenced. This suggests that the relevant crack size had been reduced by a factor of approximately 2 in the course of the polishing to 0.27 μm.

9. SUMMARY

A series of bending bars cut out from a hot isostatically pressed alumina container were investigated to determine the crack growth data in a salt solution at 70°C. The crack growth behaviour was studied in 4-point static bending tests. The results are:

- The Weibull parameters of the inert bending strength distribution are $m = 10.4$; $\sigma_o = 369$ MPa, $\hat{\sigma}_c = 355$ MPa;

- Lifetime measurements yield a low crack growth exponent of $n = 20$ obtained by evaluation of the relation $\hat{t}_f = f(\sigma)$;

- A new method was applied to determine the v-K_I-relationship from lifetime measurements.

- The v-K_I-curve can be expressed by a power law down to crack growth rates of 10^{-11} m/s with an exponent of $n = 19$.

- An analysis of Weibull moduli m_t confirms those surprisingly low n-values.

- The influence of R-curve effects on n-values measured in DT-tests is discussed on the basis of results published in the literature.

- A formula is given to allow lifetime predictions for different failure probabilities.

- Finally, the influence of surface quality on bending strength is mentioned to give an impression of attainable strength data.

10. REFERENCES

/1/ The Swedish Corrosion Institute and its Reference Group: "Aluminium oxide as an encapsulation material for unreprocessed nuclear fuel waste - evaluation from the viewpoint of corrosion"
Technical Report 80-15, KBS, Stockholm 1980.

/2/ P. Fournier, F. Naudin: "Essai de K_{Ic} et détermination du diagramme (K_I, v) du verre par la méthode de la double torsion".
Rev. Phys. Appl. 12 (1977), pp. 797 - 802.

/3/ T.E. Adams, D.J. Landini, C.A. Schumacher, B.C. Bradt: "Micro-and macrocrack growth in alumina refractories". Ceramic Bulletin 60 (1981), pp. 730 - 735.

/4/ F. Deuerler, R. Knehans, R. Steinbrech: "Zur Problematik der Lebensdauervorhersagen bei keramischen Werkstoffen mit R-Kurvenverhalten", Festigkeitsseminar MPI-Stuttgart, March 1985.

/5/ R.J. Charles, "Dynamic Fatigue of Glass", Journ. of Appl. Phys. 29 (1958), pp. 1657 - 1661.

/6/ T. Fett, D. Munz: "Determination of v-K_I-curves by a modified evaluation of lifetime measurements in static bending tests", to be published in Communications of the Amer. Ceram. Soc.

/7/ E. Kreiszig: "Statistische Methoden und ihre Anwendungen". Vandenhoek & Ruprecht, Göttingen, 1979.

/8/ S. Sclosa, D.F. Dailly, G.W. Hastings, "Fracture Toughness of Hot Isostatically Pressed Alumina", Trans. J. Br. Ceram. Soc. 81 (1982), pp. 148 - 151.

/9/ W. Hermansson: "Determination of slow crack growth in isostatically pressed Al_2O_3"
in: Ref. /1/

11. FIGURES

Fig. 1: Schematic of lifetimes ranked in increasing order as a function of initial load.

Fig. 2: v-K_I-curve evaluated from lifetime measurements shown in Fig. 1.

Fig. 3: Inert bending strength σ_c measured in dynamic 4-point bending tests in air with $\dot{\sigma}$ = 350 MPa/s.

Fig. 4: Lifetimes t_f measured in static 4-point bending tests in salt solution.

Fig. 5: Median values $\hat{t}_f$ of lifetimes from Fig. 4 in dependence of applied bending stresses σ.

Fig. 6: Individual lifetimes t_f from Fig. 4 in dependence of applied bending stresses σ normalized on individual inert strength σ_c.

Fig. 7: v-K_I-relationship obtained from data of Fig. 6 by application of Eq. (17).

Fig. 8: Nomograph for lifetime predictions.

Fig. 9: Influence of surface quality on bending strength
□ maximum peak-to-valley height 3.5 μm (mean value 0.27 μm)
■ maximum peak-to-valley height 0.046 μm (mean value 0.004 μm).

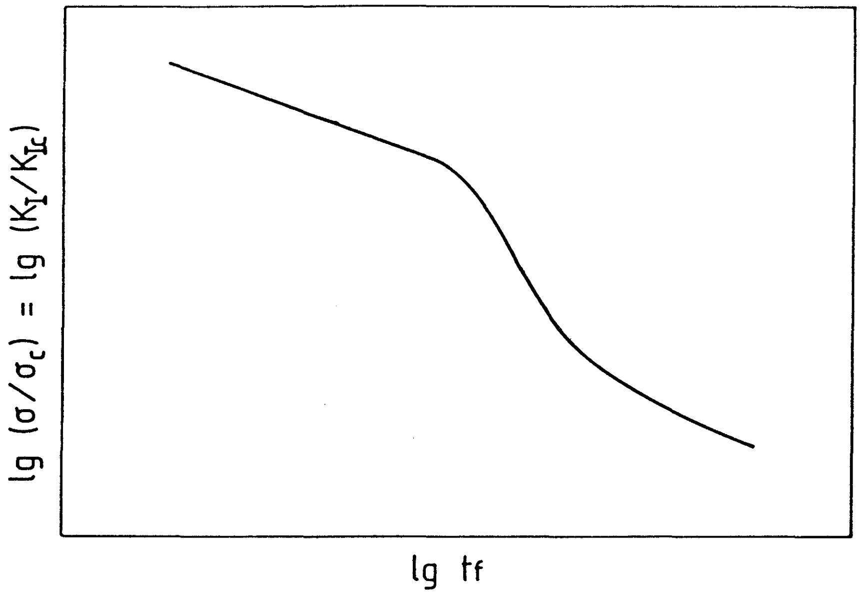

Fig. 1: Schematic of lifetimes ranked in increasing order as a function of initial load.

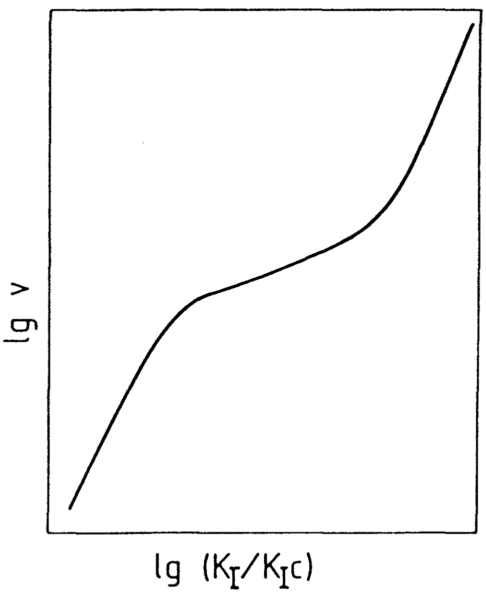

Fig. 2: v-K_I-curve evaluated from lifetime measurements shown in Fig. 1.

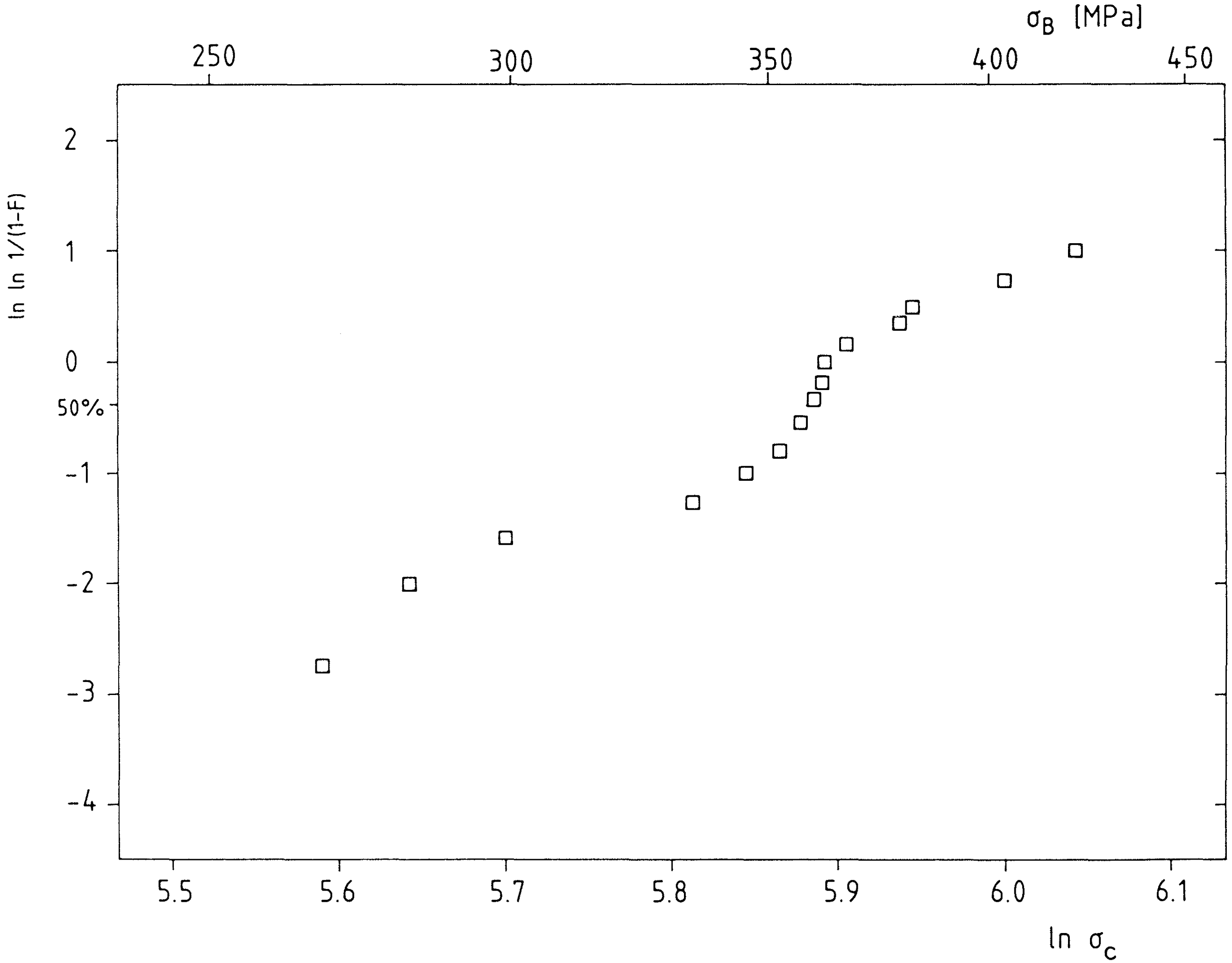

Fig. 3: Inert bending strength σ_c measured in dynamic 4-point bending tests in air with $\dot{\sigma} = 350$ MPa/s.

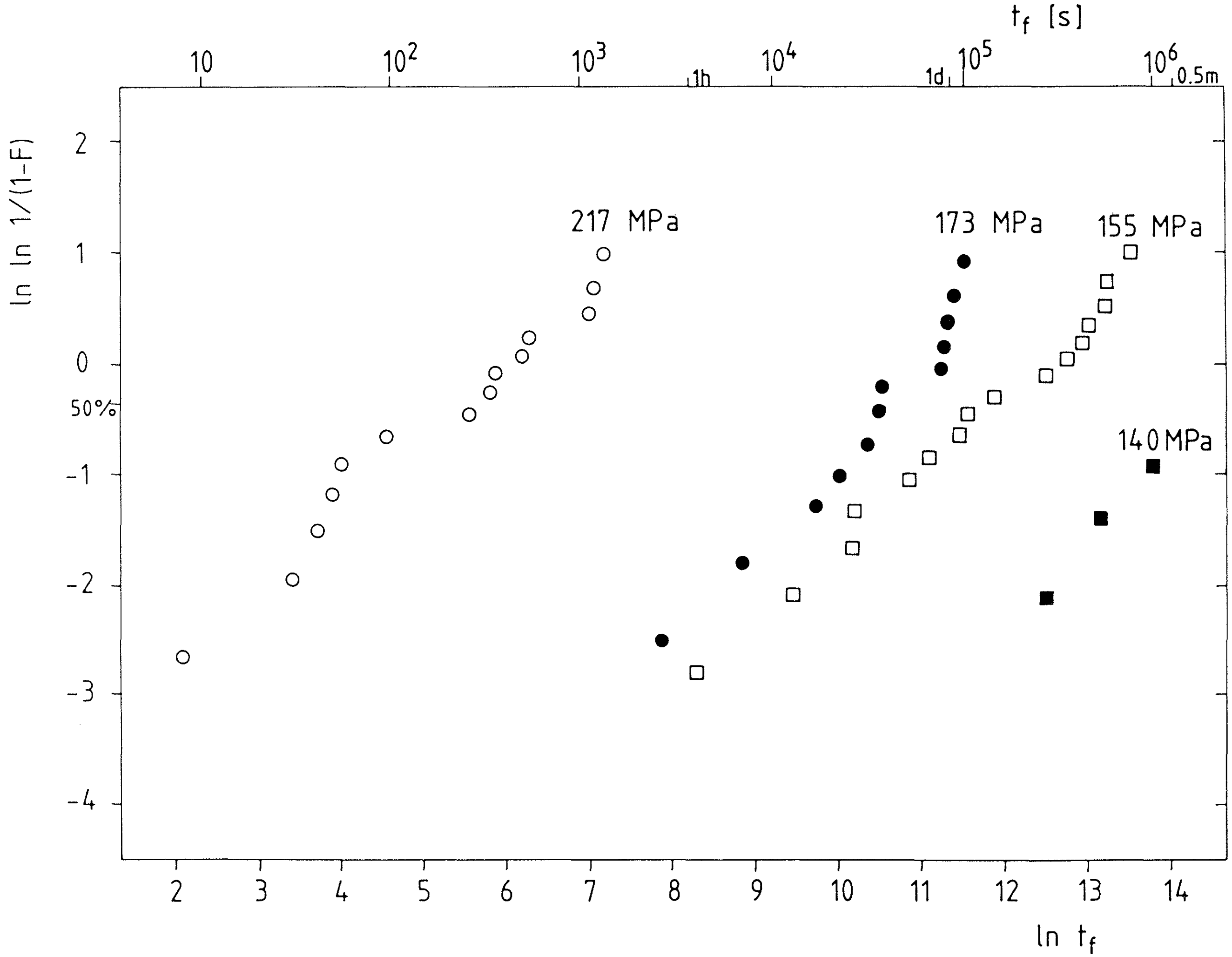

Fig. 4: Lifetimes t_f measured in static 4-point bending tests in salt solution.

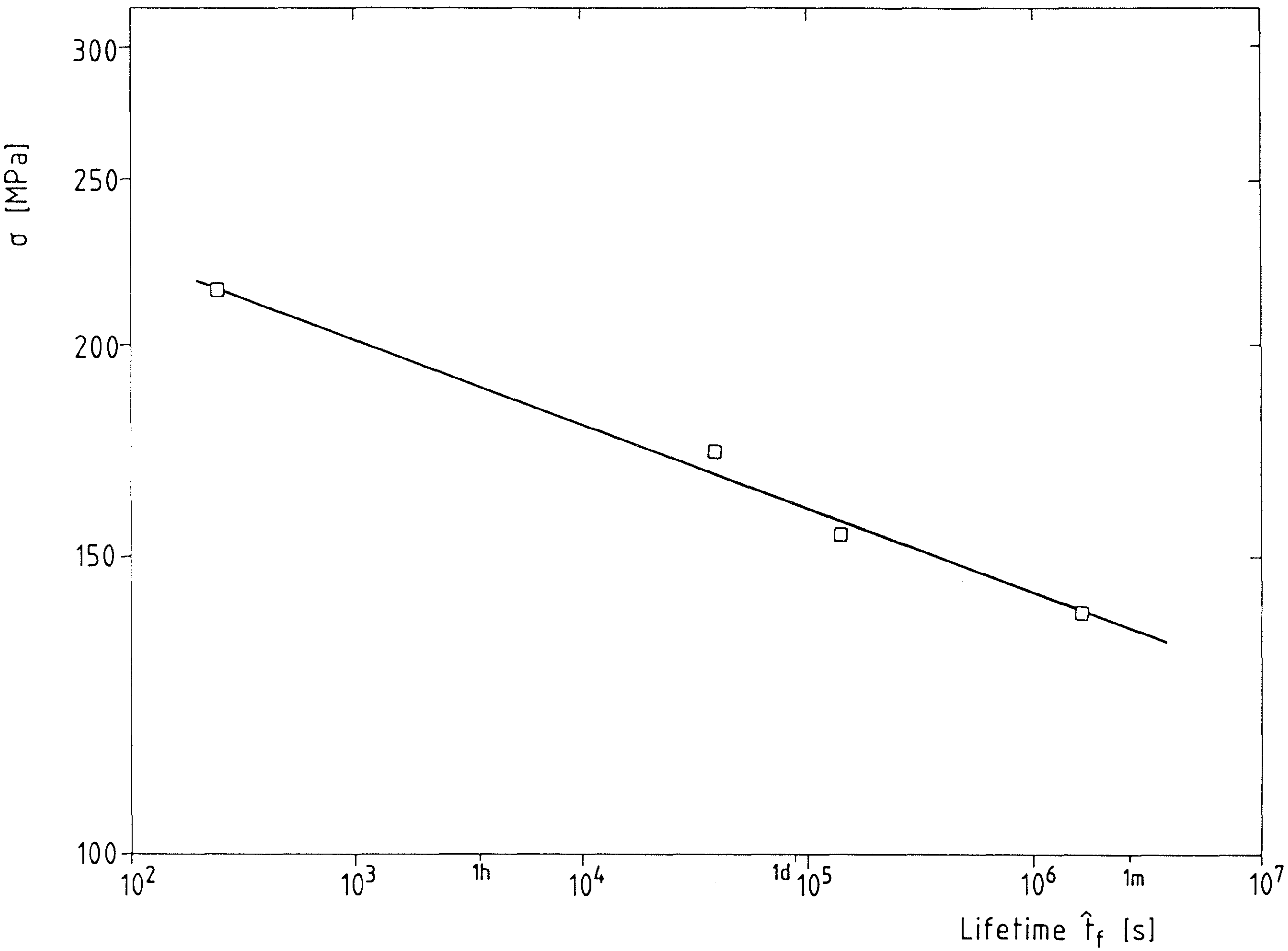

Fig. 5: Median values $\hat{t}_f$ of lifetimes from Fig. 4 in dependence of applied bending stresses σ.

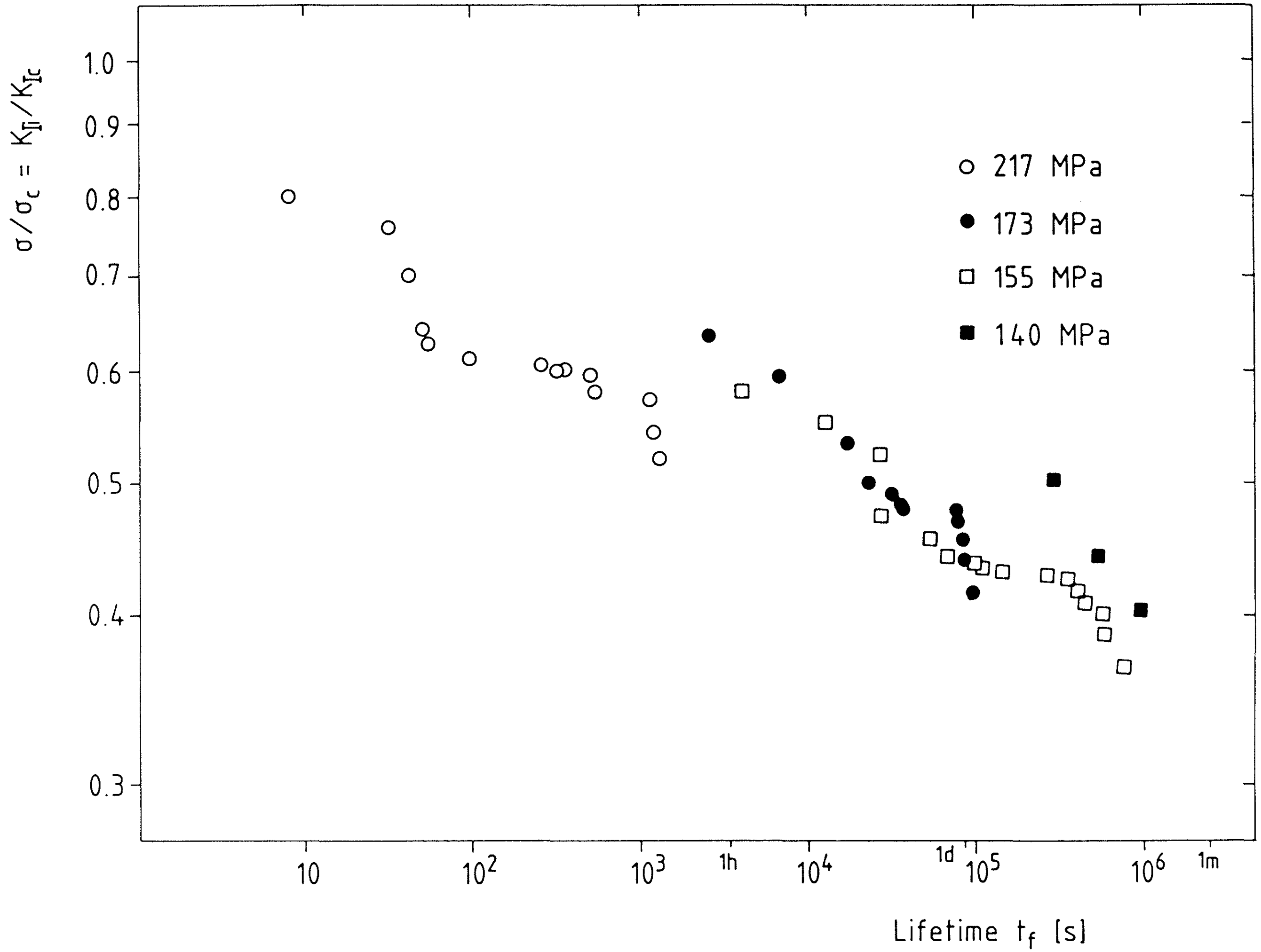

Fig. 6: Individual lifetimes t_f from Fig. 4 in dependence of applied bending stresses σ normalized on individual inert strength σ_c.

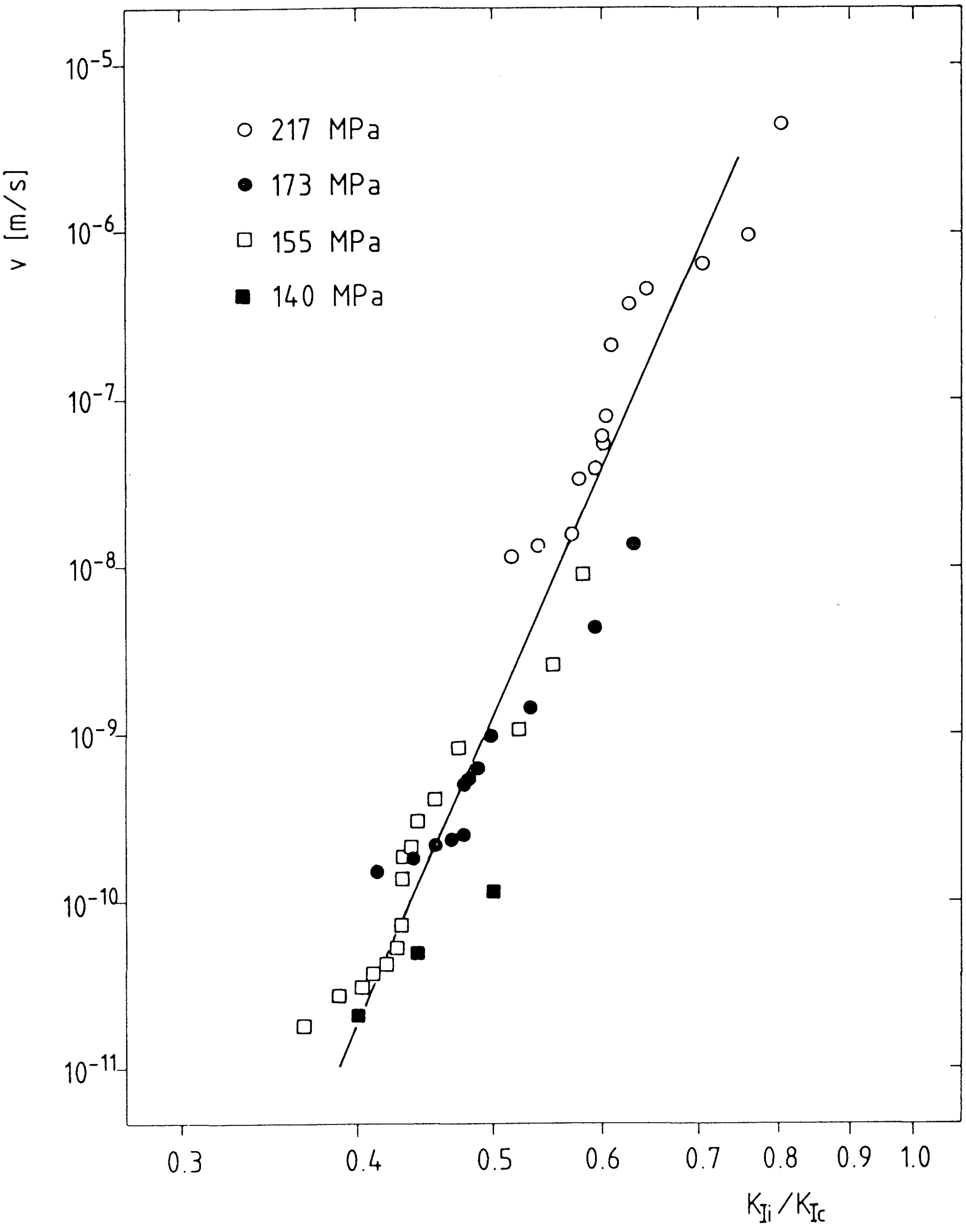

Fig. 7: v-K_I-relationship obtained from data of Fig. 6 by application of Eq. (17).

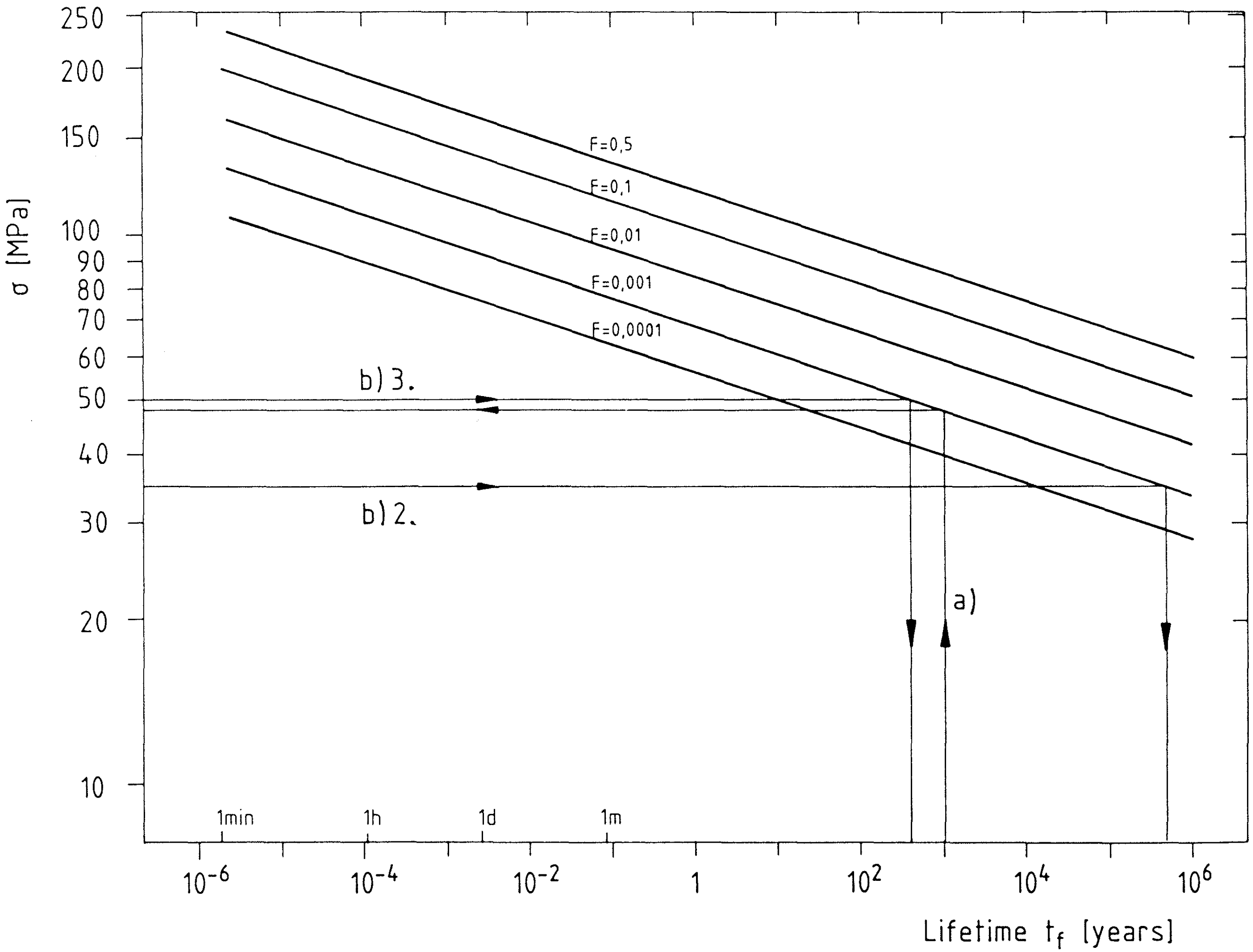

Fig. 8: Nomograph for lifetime predictions.

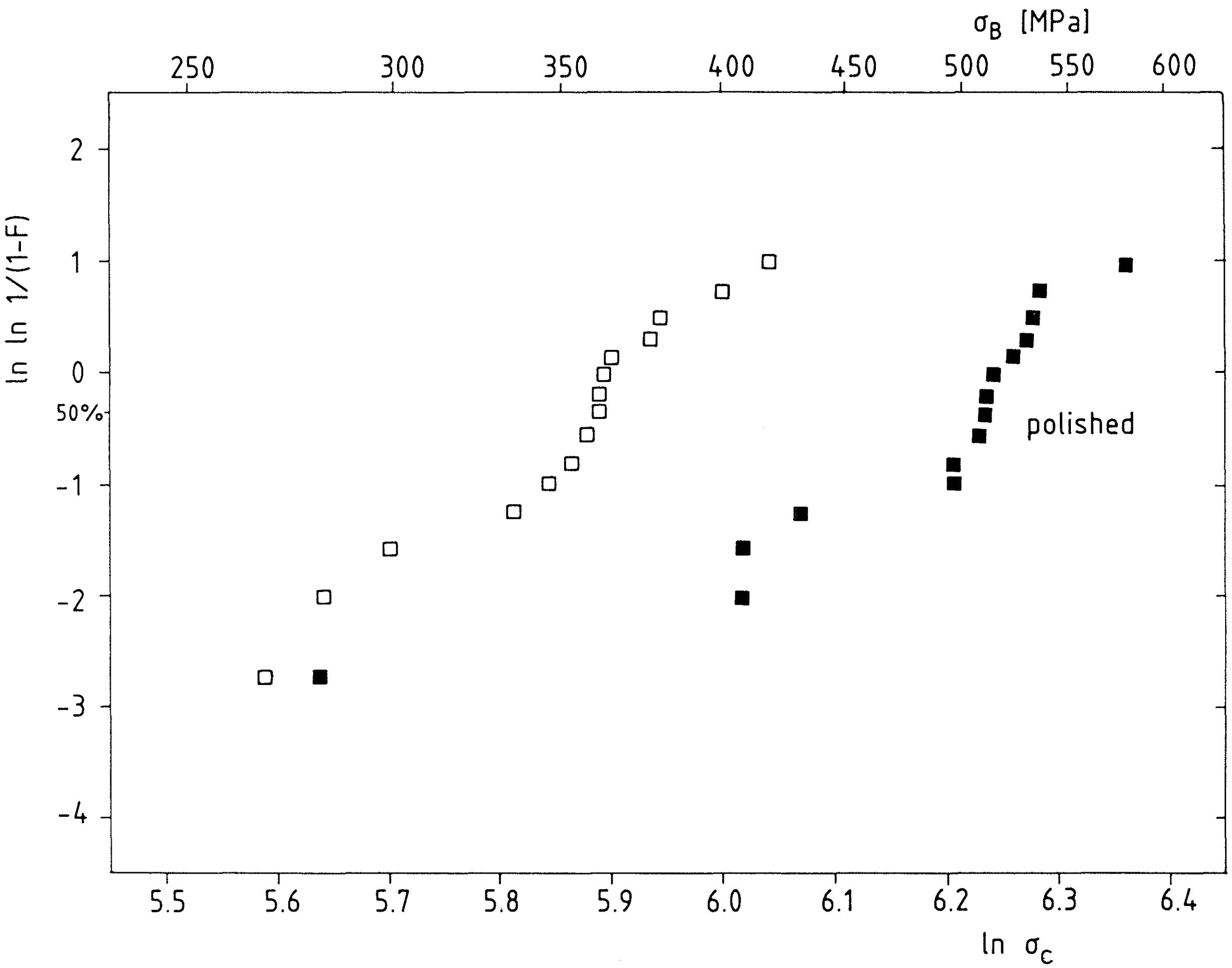

Fig. 9: Influence of surface quality on bending strength
□ maximum peak-to-valley height 3.5 μm (mean value 0.27 μm)
■ maximum peak-to-valley height 0.046 μm (mean value 0.004 μm).